Chemical Engineering & Technology Research Article

Arash Sadeghi[1]
Alireza Hemmati[2]
Mehdi Ghadiri[3,*]
Saeed Shirazian[1]

Mathematical Modeling and Simulation of Propylene Absorption Using Membrane Contactors

Separation of light olefin-paraffin mixtures having the same carbon number is one of the most energy-intensive separation processes in petrochemical industry. Gas-liquid membrane contactors as an alternative to conventional processes have gained increasing interest due to low energy consumption. A 2D comprehensive model was developed to predict the transport and chemical absorption of propylene in a cocurrent microporous membrane contactor. Formations of a complex between propylene and silver ion and dissolution of silver nitrate were considered. With increasing gas flow rate the system efficiency decreases due to the reduction of propylene residence time inside the contactor. As the absorbent amount increases in the tube, both propylene and complex penetrate more deeply into the liquid and a diffusion layer is formed near the gas-liquid interface.

Keywords: Absorption, Computational fluid dynamics, Mass transfer, Mathematical modeling, Membrane contactors

Received: April 12, 2016; *revised:* February 10, 2017; *accepted:* April 26, 2017

DOI: 10.1002/ceat.201600225

1 Introduction

Ethylene and propylene are considered as the main feedstocks of petrochemicals plants to produce valuable petrochemical products [1]. The global production of propylene has reached over 84 billion pounds per year [2]. However, there are some impurities in the light olefins streams especially ethane and propane that result in predominant issues such as reduction of productivity of polyolefin reactors [3, 4]. Separation and purifications processes are in operation at petrochemical industries in order to mitigate the problems associated with impurities. Cryogenic distillation is the main and reliable method for separation of propylene and propane while it is highly energy-intensive and has a low efficiency because of the marginal differences in relative volatility of propylene and propane [5, 6]. To reduce energy consumption in this particular application and to develop a system with reasonable apparatus size, membrane technology has been considered as a viable alternative for separation of propylene from propane [7].

Extensive research has been done on various kinds of membranes including carbon molecular sieves [8], polymers [9], zeolites [10], and facilitated transport membranes [11]. Polymeric and polymeric-composite membranes are one of the major interesting media which are studied in propylene separation from an olefin-paraffin mixture. Polymeric membranes are commonly used in membrane contactor systems [12] in which the porous membrane is employed for contacting two phases. Membrane contactors have gained special attention as an alternative technology due to numerous benefits including straightforward scale-up, high gas-liquid interfacial area, undisturbed available surface area at different flow rates, etc. [13, 14].

Membrane contactor systems in gas-liquid and liquid-liquid applications have three distinct subdomains consisting of lumen, membrane, and shell. For gas absorption by a liquid, a gas stream enters on one side of a hydrophobic microporous membrane while an absorbent enters on the other side. The liquid is not able to penetrate through the membrane pores due to the hydrophobic nature of the membrane. Therefore, a gas-liquid interface is formed at the pore openings adjacent to the liquid phase in the membrane module. Gas species penetrate from the gas side across the membrane and reach the gas-liquid interface, where the gas species is absorbed in the liquid and then diffuses into another subdomain [15]. Therefore, mass transfer and transport of species from one side to other side in these systems are highly important for modeling of membrane contactor systems. The mass transfer of propylene

[1]Arash Sadeghi, Dr. Saeed Shirazian
Department of Chemical Sciences, Bernal Institute, Analog Devices Building, University of Limerick, Castletroy, Limerick, Ireland.

[2]Dr. Alireza Hemmati
Department of Chemical Engineering, Faculty of Engineering, South Tehran Branch, Islamic Azad University, Ahang St., P.O. Box 19585-466, Tehran, Iran.

[3]Mehdi Ghadiri
m_ghadiri10@yahoo.com
Young Researchers and Elite Club, South Tehran Branch, Islamic Azad University, Tehran, Iran.

is theoretically investigated in the current research with the focus on a comprehensive and reliable model.

Several correlations between experimental data and modeling values have been proposed due to the importance of mass transfer. It should be noted that modeling and simulation reduce the expense of process optimization at industrial scale [16]. Qi and Cussler [17] developed a theory of the operation of a hollow-fiber membrane contactor in terms of mass transfer coefficients in the liquid phase, as well as overall mass transfer coefficients. Numerous studies have been performed on CO_2 absorption using membrane contactors in gas-liquid mode of operation. A 2D mathematical model was developed for the physical absorption of CO_2 in hollow-fiber membrane contactors by Al-Marzouqi et al. [18]. They studied the effect of operating parameters including different gas and liquid flow rates, gas-to-liquid ratios, and temperatures on the removal of CO_2.

One of the most important methods is the resistance-in-series model. In this approach, the resistances in the three compartments of the membrane contactor are considered in series and the process is modeled based on the resistances [19]. In recent years, computational fluid dynamics (CFD) has been used to simulate mass transfer in membrane contactors. The affecting parameters of the system are determined in a very small part of the module; therefore, it is possible to investigate the transport phenomena in the membrane contactors in an appropriate way [20]. This method was applied by a number of researchers to model hollow-fiber membrane contactors in various processes such as membrane-based solvent extraction and membrane distillation [21, 22]. This approach relies on solving conservation equations including momentum, continuity, and energy equations [23]. However, only few studies reported on the propylene separation from propane, so there is a definite need for developing this process.

The major aim of the current investigation is to develop and solve a 2D mathematical model for chemical absorption of propylene from pure gas into silver nitrate solution in hollow-fiber membrane contactors. The model considers axial and radial diffusion in the lumen, microporous membrane, and shell side of the contactor, convection in the lumen and shell as well as formation of complex between propylene and silver ion, and silver nitrate dissolution.

2 Model Development

2.1 Chemistry of Process

Propylene (a) penetrates through the membrane pores and dissolves in the liquid phase. It reacts with a silver ion (b) according to the following reaction [24]:

$$C_3H_6(a) + Ag^+(b) \rightleftharpoons C_3H_6{-}Ag^+(c) \quad (1)$$

where a–c refer to the species for simplicity. Also, silver nitrate ($AgNO_3$) dissociates in the liquid phase as follows:

$$AgNO_3(d) \rightleftharpoons Ag^+(b) + NO_3^-(n) \quad (2)$$

The equilibrium constants for Eqs. (1) and (2) can be written as:

$$K_c = \frac{k_1}{k_2} = \frac{[C_3H_6{-}Ag^+]}{[C_3H_6][Ag^+]} \quad (3)$$

$$K_{diss} = \frac{k_3}{k_4} = \frac{[Ag^+][NO_3^-]}{[AgNO_3]} \quad (4)$$

The reaction rate of propylene, silver ion, formed complex (C_3H_6-Ag^+), and silver nitrate in the lumen side are given as follows [24]:

$$R_{a,lumen} = -k_1 C_a C_b + k_2 C_c \quad (5)$$

$$R_{b,lumen} = -k_1 C_a C_b + k_2 C_c + k_3 C_d - k_4 C_b (C_b + C_c) \quad (6)$$

$$R_{c,lumen} = k_1 C_a C_b - k_2 C_c \quad (7)$$

$$R_{d,lumen} = -k_3 C_d + k_4 C_b (C_b + C_c) \quad (8)$$

where C[1)] refers to the concentration of a particular species in mol m^{-3}.

2.2 Model Equations

Fig. 1 shows a schematic of the membrane extractor with a hydrophobic microporous membrane which divides the system into two main subchannels, i.e., lumen and shell. The liquid

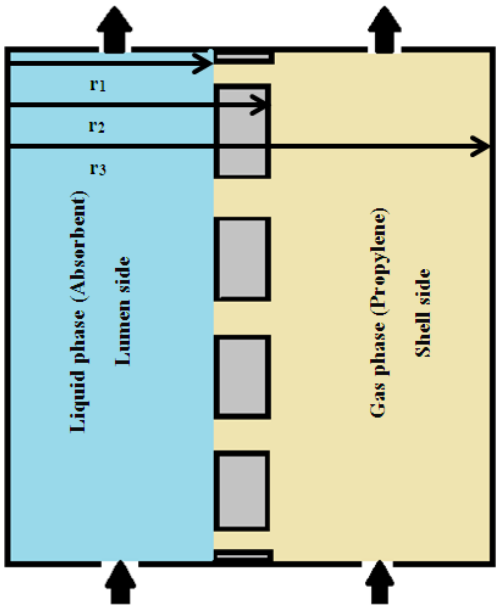

Figure 1. Cross-sectional area of the membrane contactor.

1) List of symbols at the end of the paper.

phase containing silver nitrate flows in the lumen side, while the pure propylene flows cocurrently inside the shell. Due to the hydrophobicity of the fiber, the gas phase penetrates the membrane pores and fills them. The latter is known as non-wetted mode in literature.

The mass transfer model for prediction of the process is built considering the following assumptions: (1) steady-state and isothermal conditions for both phases, i.e., gas and liquid; (2) fully developed parabolic velocity profile for the liquid phase inside the fiber; (3) laminar flow regime for the two phases in the contactor; and (4) the membrane is completely gas-phase-filled because the membrane is highly hydrophobic and the solvent is not able to fill the membrane pores.

A continuity equation is defined as the main equation to predict the transfer of propylene from the gas phase to the liquid phase. This equation is derived from the mass balance of propylene within an infinitesimal region (control volume). The differential form of the continuity equation can be expressed as follows [25]:

$$\frac{\partial C_i}{\partial t} + \nabla(-D_i \nabla C_i + C_i V) = R_i \tag{9}$$

where C_i is the concentration of component i, D_i denotes the component diffusion coefficient, V is the liquid velocity in the tube, and R_i is the reaction term. The continuity equation is considered in the three subdomains of the model (Fig. 1).

2.2.1 Lumen Side

The steady-state continuity equation for transport of propylene, silver ion, formed complex (C_3H_6-Ag^+), and silver nitrate in the lumen side of the membrane contactor can be written as [25]:

$$D_{a,lumen}\left[\frac{\partial^2 C_{a,lumen}}{\partial r^2} + \frac{1}{r}\frac{\partial C_{a,lumen}}{\partial r}\frac{\partial^2 C_{a,lumen}}{\partial z^2}\right] = V_{z,lumen}\frac{\partial C_{a,lumen}}{\partial z} - k_1 C_a C_b + k_2 C_c \tag{10}$$

$$D_{b,lumen}\left[\frac{\partial^2 C_{b,lumen}}{\partial r^2} + \frac{1}{r}\frac{\partial C_{b,lumen}}{\partial r}\frac{\partial^2 C_{b,lumen}}{\partial z^2}\right] = V_{z,lumen}\frac{\partial C_{b,lumen}}{\partial z} - k_1 C_a C_b + k_2 C_c + k_3 C_d - k_4 C_b (C_b + C_c) \tag{11}$$

$$D_{c,lumen}\left[\frac{\partial^2 C_{c,lumen}}{\partial r^2} + \frac{1}{r}\frac{\partial C_{c,lumen}}{\partial r}\frac{\partial^2 C_{c,lumen}}{\partial z^2}\right] = V_{z,lumen}\frac{\partial C_{c,lumen}}{\partial z} + k_1 C_a C_b - k_2 C_c \tag{12}$$

$$D_{d,lumen}\left[\frac{\partial^2 C_{d,lumen}}{\partial r^2} + \frac{1}{r}\frac{\partial C_{d,lumen}}{\partial r}\frac{\partial^2 C_{d,lumen}}{\partial z^2}\right] = V_{z,lumen}\frac{\partial C_{d,lumen}}{\partial z} - k_3 C_d + k_4 C_b (C_b + C_c) \tag{13}$$

A velocity distribution is required to solve the continuity equations. The velocity distribution in the lumen side was assumed to follow the Newtonian laminar flow as follows:

$$V_{z,lumen} = 2u\left[1 - \left(\frac{r}{r_1}\right)^2\right] \tag{14}$$

where u is the average fluid velocity in the lumen side, r is the radial coordinate, and r_1 is the inner radius of the lumen. It should be pointed out that the convection term in the mass transfer equations in radial direction is neglected because the velocity of the liquid phase is in axial direction and the contribution of this term is negligible.

2.2.2 Membrane Side

The steady-state mass transfer for the transport of propylene inside the membrane pores for non-wetted condition, which is considered to be due to diffusion only, can be written as [25]:

$$D_{a,membrane}\left[\frac{\partial^2 C_{a,membrane}}{\partial r^2} + \frac{1}{r}\frac{\partial C_{a,membrane}}{\partial r}\frac{\partial^2 C_{a,membrane}}{\partial z^2}\right] = 0 \tag{15}$$

2.2.3 Shell Side

The steady-state form of the mass transfer equation for the transport of propylene in the shell side, where the gas stream flows, is defined as:

$$D_{a,shell}\left[\frac{\partial^2 C_{a,shell}}{\partial r^2} + \frac{1}{r}\frac{\partial C_{a,shell}}{\partial r}\frac{\partial^2 C_{a,shell}}{\partial z^2}\right] = V_{z,shell}\frac{\partial C_{a,shell}}{\partial z} \tag{16}$$

Velocity distribution should be coupled with the mass transfer equation. It is required for solving the mass transfer equation (Eq. (16)). Therefore, the Navier-Stokes equations are considered for describing the velocity filed in the shell side. It can be expressed as follows [25]:

$$-\nabla\eta\left(\nabla V_{z,shell} + (\nabla V_{z,shell})^T\right) + \rho(V_{z,shell}\nabla)V_{z,shell} + \nabla p = 0$$
$$\nabla V_{z,shell} = 0 \tag{17}$$

where η, ρ, and p refer to viscosity, density, and pressure of the gas mixture, respectively. Density and viscosity of the modeled fluids are constant, which yields a continuity condition. Boundary conditions for the equations are listed in Tab. 1 where m is the physical solubility of propylene in the liquid phase.

2.3 Numerical Solution of Model Equations

The equations related to lumen, microporous membrane, and shell sides with the boundary conditions as listed in Tab. 1 were

Table 1. Boundary conditions for the model's equations.

Position	Shell	Membrane	Tube (lumen)
$z = 0$	$C_a = C_{a0}$, $V = V_{inlet}$	Insulated	$C_a = 0$, $C_b = C_{b0}$, $C_c = 0$, $C_d = C_{d0}$
$z = L$	Convective flux, $p = p_{atm}$	Insulated	Convective flux for all equations
$r = 0$	–	–	Axial symmetry
$r = r_1$	–	$C_{a,m} = C_{a,t}/m$	$C_{a,t} = C_{a,m}m$, insulated for other species
$r = r_2$	$C_{a,g} = C_{a,m}$, no slip	$C_{a,m} = C_{a,g}$	–
$r = r_3$	Insulated	–	–

solved with COMSOL Multiphysics version 4.2 software which applies the finite element method for numerical solutions of the model equations. The finite element analysis (FEM) is combined with adaptive meshing and error control using the numerical solver of UMFPACK version 4.2 of the software to solve the governing equation numerically. The parameters used in the simulations are listed in Tab. 2.

Table 2. Parameters used in the simulation of membrane contactor [24, 26].

Parameter	Value
Shell inner diameter [mm]	7
Fiber length L [mm]	250
Tube inner diameter [mm]	1
Tube outer diameter [mm]	2
Number of fibers N [–]	1
$AgNO_3$ concentration [mol m^{-3}]	1000–4000
Viscosity η [Pa s]	1×10^{-3}
D_a in the tube side [m^{2}s^{-1}]	1.06×10^{-9}
D_b in the tube side [m^{2}s^{-1}]	1.08×10^{-9}
D_c in the tube side [m^{2}s^{-1}]	8.45×10^{-10}
D_d in the tube side [m^{2}s^{-1}]	8.85×10^{-10}
D_a in the membrane side [m^{2}s^{-1}]	2×10^{-6}
D_a in the shell side [m^{2}s^{-1}]	5×10^{-6}
k_1 [m^{3}mol^{-1}s^{-1}]	600
k_2 [s^{-1}]	3448
k_3 [s^{-1}]	500
k_4 [m^{3}mol^{-1}s^{-1}]	1660
m [m^{3}kPa mol^{-1}]	$1/H$
H [mol m^{-3}kPa^{-1}]	2.82×10^{-2}

3 Results and Discussion

3.1 Model Validation

The modeling results were compared with the experimental values obtained in [24] to verify the model accuracy developed here for chemical absorption of propylene from gas streams. In the simulations, the influence of liquid-phase velocity on propylene absorption flux was taken into account to evaluate the effect of this parameter. Fig. 2 illustrates the comparison between modeling predictions and experimental data reported by Rajabzadeh et al. [24]. The propylene absorption flux could be enhanced with increasing liquid-phase (absorbent) flow rate; however, it has no considerable effect on the absorption of propylene by the liquid phase and can be neglected. The slight increase in propylene absorption could be attributed to the higher transfer coefficient with increasing the liquid flow rate [24].

3.2 Total Flux of Propylene

The direction of propylene transport in the membrane contactor is represented in Fig. 3 by arrows which indicate the mass transfer flux of propylene. Pure propylene is fed into the shell side of the membrane contactor, while a silver nitrate solution as absorbent liquid enters into the lumen side of the hollow-fiber contactor. The flow pattern in the membrane contactor is parallel and cocurrent. As the pure propylene flows through the shell side of the contactor, it moves towards the membrane surface due to the concentration gradient and then penetrates through the membrane pores where the liquid phase is not able to diffuse due to the hydrophobic nature of the microporous membrane used in this absorption process.

At the membrane-liquid interface, a chemical reaction occurs between silver ion and propylene (Eq. (1)) and a complex is formed consequently. Finally, the formed complex is swept by the moving silver nitrate solution and leaves the contactor in the lumen side. Fig. 4 confirms that the concentration decreases along the contactor because of the absorption of the propylene.

3.3 Propylene Concentration Profile in Radial Direction

The propylene concentration profile in the membrane contactor in radial direction is demonstrated in Fig. 5. There is a sharp decrease in concentration in the membrane side of the module while the concentration change is small in the lumen side. The latter is because the diffusion mechanism in the shell and tube sides is convection and diffusion, and resistance to propylene transport is small. However, the transport of propylene only occurs by diffusion mechanism inside the microporous membrane. In addition, it can be seen that there is a sharp decrease in the lumen side near the membrane surface

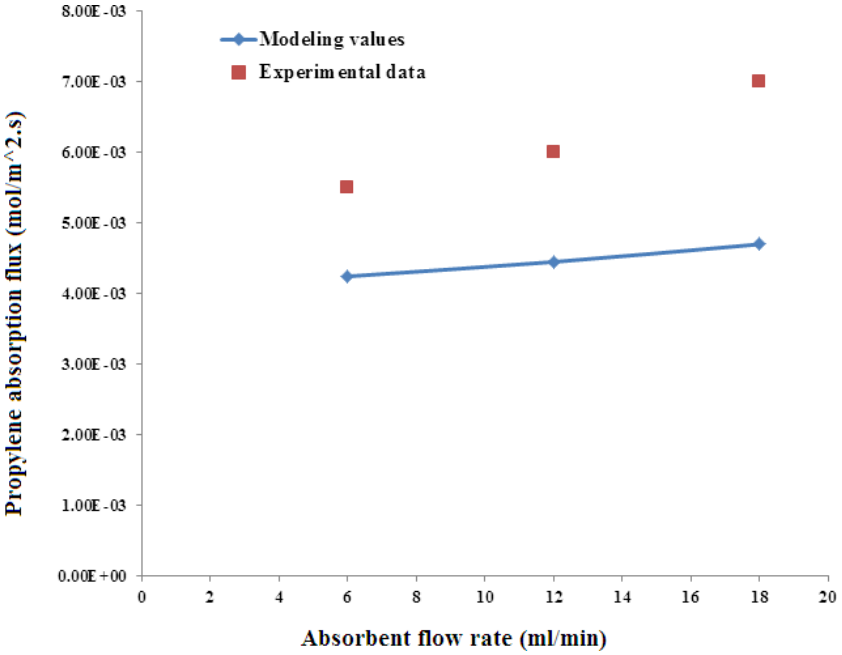

Figure 2. Propylene absorption flux vs absorbent flow rate for model validation.

which is due to the formation of a diffusion layer or boundary layer near the gas-liquid interface [24]. Therefore, the model is capable of predicting the concentration boundary layer in absorption of propylene using membrane contactors.

3.4 Concentration Distribution of Species in the Lumen Side

The concentration distribution of propylene, silver ion, and formed complex in the lumen side of membrane contactor is illustrated in Fig. 6. As the absorbent goes up in the lumen, both propylene and complex penetrate more deeply into the liquid. The silver ion is consumed by the reaction with propylene and the complex forms at the gas-liquid interface. Reversibility of the reaction leads to the small reduction in silver ion concentration. Also, the concentration distribution of propylene and complex are slightly similar because there occurs an instantaneous reversible reaction along with the very fast reaction of propylene with silver ions.

3.5 Effect of Gas-Phase Flow Rate

Fig. 7 indicates the influence of the pure propylene stream flow rate in the shell side on the chemical absorption efficiency of propylene. Increasing the feed flow rates from 20 to 40 mL min^{-1} decreases the absorption efficiency of propylene from approximately 20 to 13 % in the membrane contactor. With increasing the flow rate of the gas phase, the residence time of the gas feed in the contactor becomes shorter and, therefore, the mass transfer of propylene from gas phase to liquid phase decreases as well. The latter means that the time for contacting two phases is not sufficient to achieve a satisfactory separation/absorption.

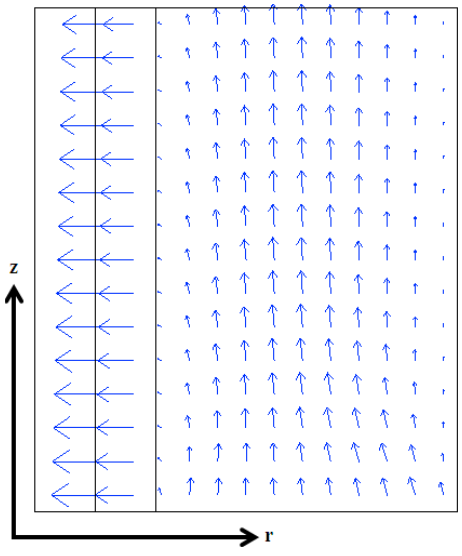

Figure 3. Arrows of total flux distribution of propylene in the contactor.

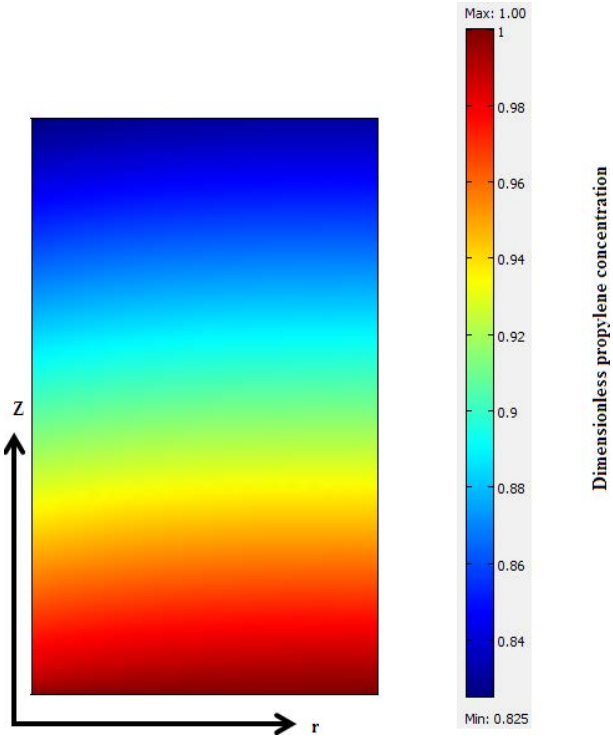

Figure 4. Dimensionless concentration distribution of propylene in the shell side of the contactor.

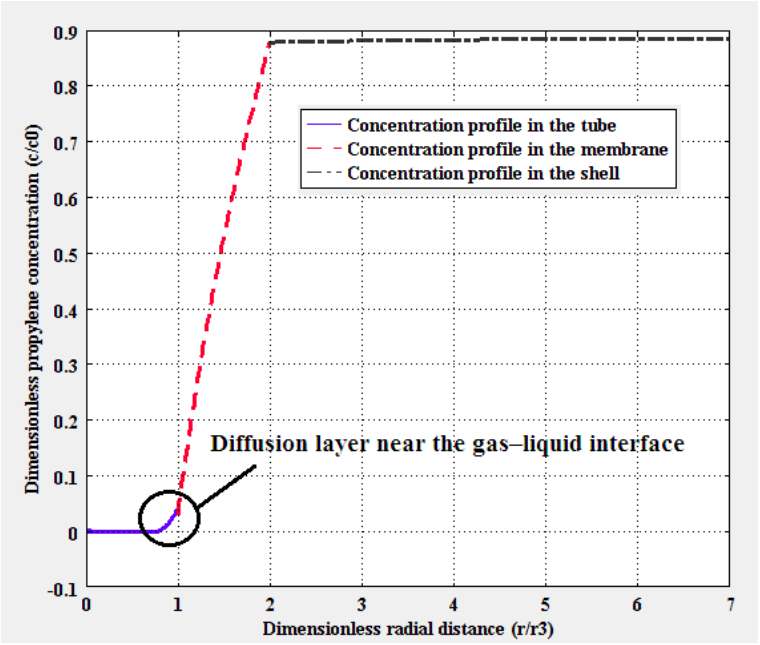

Figure 5. Propylene concentration profile in the radial direction at the middle of the membrane contactor (z/L = 0.5).

The dimensionless propylene concentration along the length of the contactor in the shell side for different values of gas flow rates is presented in Fig. 8. The concentration of propylene at the contactor outlet increases with the enhancement of the gas-phase flow rate. This also confirms that the absorption efficiency has inverse relation to the gas-phase flow rate.

4 Conclusions

Gas-liquid membrane contactors represent a novel absorber design offering several improvements over conventional absorption systems. Modeling and simulation of membrane contactors can reduce the expense of process optimization at industrial scale.

A mathematical model for pure propylene absorption in a membrane contactor was proposed. In order to achieve accurate results, all chemical reactions including complex formation between propylene and silver ions, as well as silver nitrate dissolution were taken into account in the model development. Concentration distribution of propylene, silver ions, and formed complex were determined and the effect of gas and liquid phases on absorption efficiency was investigated. It was concluded that a higher flow rate of the liquid phase has no significant effect on propylene absorption while an enhanced gas-phase flow rate decreases propylene absorption due to the reduction of residence time. Also, the diffu-

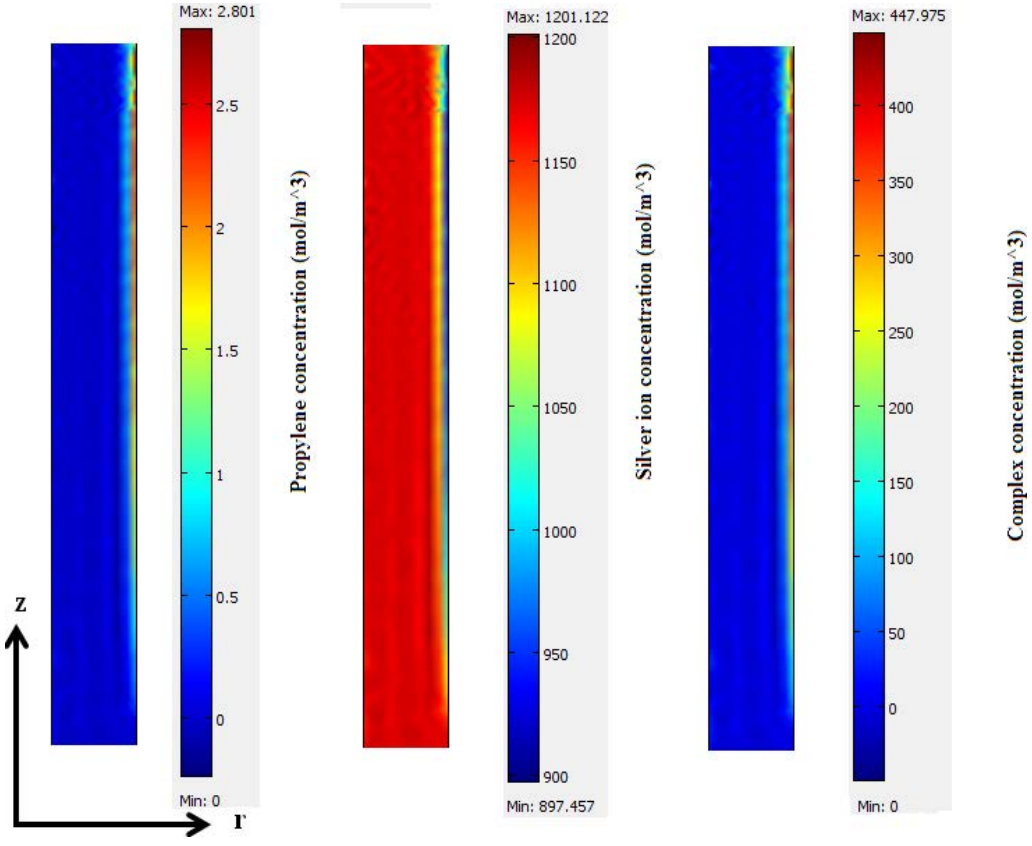

Figure 6. Concentration distribution of propylene, silver ion, and formed complex in the lumen side of membrane contactor.

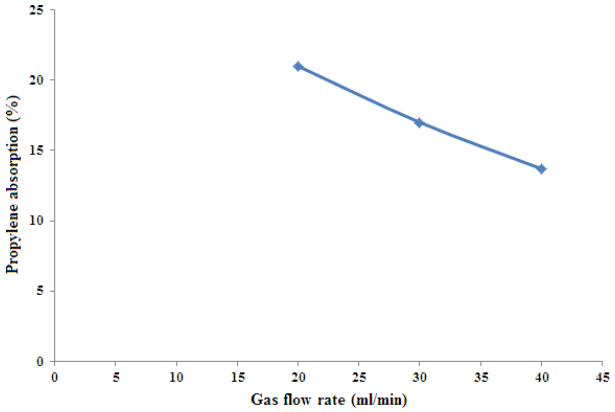

Figure 7. Effect of gas-phase flow rate in the shell side of the membrane contactor on propylene absorption efficiency.

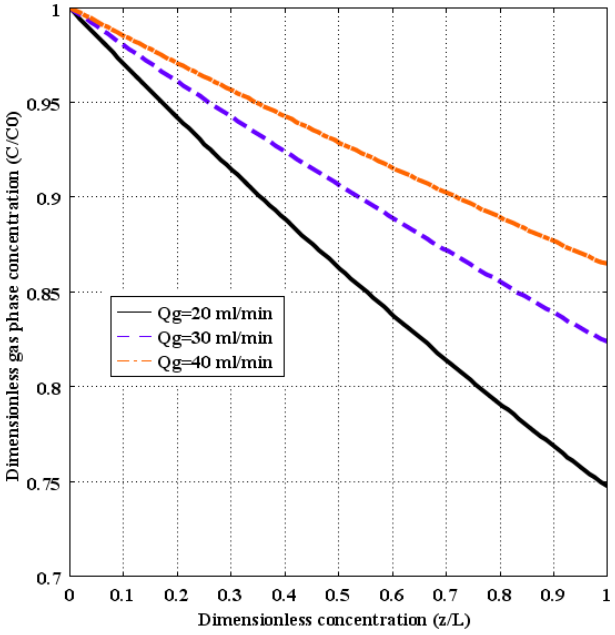

Figure 8. Dimensionless propylene concentration in the shell side along the length of the contactor at different gas-phase flow rates.

sion layer adjacent to the gas-liquid interface can be determined applying the current simulation methodology.

The authors have declared no conflict of interest.

Symbols used

C_i	[mol m^{-3}]	concentration of species *i*
D_i	[m^{2}s^{-1}]	diffusivity of species *i*
H	[mol m^{-3}kPa^{-1}]	Henry's constant
k_1	[m^{3}mol^{-1}s^{-1}]	reaction rate constant of Eq. (1)
k_2	[s^{-1}]	reaction rate constant of reverse Eq. (1)
k_3	[s^{-1}]	dissociation rate constant of Eq. (2)
k_4	[m^{3}mol^{-1}s^{-1}]	reaction rate constant of reverse Eq. (2)
K_c	[–]	chemical equilibrium constant of Eq. (1)
K_{diss}	[mol m^{-3}]	dissociation constant of Eq. (2)
L	[m]	fiber length
m	[–]	physical solubility of propylene in liquid phase
N	[–]	number of fibers
p	[Pa]	pressure
Q	[ml min^{-1}]	volumetric flow rate
R	[–]	reaction rate
r	[m]	radial coordinate
r_1	[m]	inner radius of hollow fiber
r_2	[m]	outer radius of hollow fiber
r_3	[m]	inner radius of shell
t	[s]	time
T	[K]	temperature
u	[m s^{-1}]	average liquid velocity
V	[m s^{-1}]	liquid velocity in the tube
z	[m]	axial coordinate

Greek letters

η	[Pa s]	viscosity of the gas mixture
ρ	[kg m^{-3}]	density of the gas mixture

Subscripts

a	C_3H_6
b	Ag^+
c	C_3H_6-Ag^+ complex
d	$AgNO_3$
g	gas phase
m	membrane
n	NO_3^-
t	tube side

Abbreviations

CFD	computational fluid dynamics
FEM	finite element method

References

[1] D. F. Sanders, Z. P. Smith, R. Guo, L. M. Robeson, J. E. McGrath, D. R. Paul, B. D. Freeman, *Polymer* **2013**, *54*, 4729.
[2] W. J. Koros, R. P. Lively, *AIChE J.* **2012**, *58*, 2624.
[3] R. Faiz, K. Li, *Desalination* **2012**, *287*, 82.
[4] R. J. Swaidan, X. Ma, E. Litwiller, I. Pinnau, *J. Membr. Sci.* **2015**, *495*, 235.
[5] R. B. Eldridge, *Ind. Eng. Chem. Res.* **1993**, *32*, 2208.
[6] D. C. Nymeijer, T. Visser, R. Assen, M. Wessling, *Sep. Purif. Technol.* **2004**, *37*, 209.
[7] S. Azizi, T. Kaghazchi, A. Kargari, *J. Taiwan Inst.Chem. Eng.* **2015**, *57*, 1.
[8] A. B. Fuertes, I. Menendez, *Sep. Purif. Technol.* **2002**, *28*, 29.
[9] C. Staudt-Bickel, W. J. Koros, *J. Membr. Sci.* **2000**, *170*, 205.
[10] N. Hara, M. Yoshimune, H. Negishi, K. Haraya, S. Hara, T. Yamaguchi, *J. Membr. Sci.* **2014**, *450*, 215.

[11] S. W. Kang, J. H. Kim, K. Char, J. Won, Y. S. Kang, *J. Membr. Sci.* **2006**, *285*, 102.
[12] S. Sridhar, A. A. Khan, *J. Membr. Sci.* **1999**, *159*, 209.
[13] A. Gabelman, S. T. Hwang, *J. Membr. Sci.* **1999**, *159*, 61.
[14] X. Wang, J. Gao, J. Zhang, X. Zhang, R. Guo, *Chem. Eng. Technol.* **2015**, *38*, 215.
[15] M. Rezakazemi, Z. Niazi, M. Mirfendereski, S. Shirazian, T. Mohammadi, A. Pak, *Chem. Eng. J.* **2011**, *168*, 1217.
[16] M. Farjami, A. Moghadassi, V. Vatanpour, *Chem. Eng. Process.* **2015**, *98*, 41.
[17] Z. Qi, E. L. Cussler, *J. Membr. Sci.* **1985**, *23*, 321.
[18] M. H. Al-Marzouqi, M. H. El-Naas, S. A. M. Marzouk, M. A. Al-Zarooni, N. Abdullatif, R. Faiz, *Sep. Purif. Technol.* **2008**, *59*, 286.
[19] M. Fallanza, A. Ortiz, D. Gorri, I. Ortiz, *J. Membr. Sci.* **2011**, *385–386*, 217.
[20] H. Haghshenas, M. T. Sadeghi, M. Ghadiri, *Chem. Eng. Process.* **2016**, *102*, 194.
[21] M. Ghadiri, S. Shirazian, *Chem. Eng. Process.* **2013**, *69*, 57.
[22] M. Ghadiri, S. Fakhri, S. Shirazian, *Ind. Eng. Chem. Res.* **2013**, *52*, 3490.
[23] M. Ghadiri, V. Abkhiz, M. Parvini, A. Marjani, *Chem. Eng. Technol.* **2014**, *37*, 543.
[24] S. Rajabzadeh, M. Teramoto, M. H. Al-Marzouqi, E. Kamio, Y. Ohmukai, T. Maruyama, H. Matsuyama, *J. Membr. Sci.* **2010**, *346*, 86.
[25] R. B. Bird, W. E. Stewart, E. N. Lightfoot, *Transport Phenomena*, 2nd ed., John Wiley & Sons, New York **2002**.
[26] R. C. Reid, J. M. Prausnitz, B. E. Poling, *The Properties of Gases and Liquids*, 4th ed., McGraw-Hill, New York **1987**.

Research Article: Gas-liquid membrane contactors are an energy-saving alternative to conventional processes for separation of light olefin-paraffin mixtures having the same carbon number. Such separation process using membrane technology is simulated by means of a computational fluid dynamics approach. Modeling and simulation can reduce the expense of process optimization at industrial scale.

Mathematical Modeling and Simulation of Propylene Absorption Using Membrane Contactors

A. Sadeghi, A. Hemmati, M. Ghadiri*, S. Shirazian

Chem. Eng. Technol. **2017**, *40 (XX)*, XXX … XXX

DOI: 10.1002/ceat.201600225